Color Erasure Detectors Enable Chromatic Interferometry

Luo-Yuan Qu,[1,2,3] Jordan Cotler,[4] Fei Ma,[1,2,3] Jian-Yu Guan,[1,2] Ming-Yang Zheng,[3] Xiuping Xie,[3] Yu-Ao Chen,[1,2] Qiang Zhang,[1,2,3] Frank Wilczek,[5,6,7,8,9] and Jian-Wei Pan[1,2]

[1]*Shanghai Branch, National Laboratory for Physical Sciences at Microscale and Department of Modern Physics University of Science and Technology of China, Shanghai 201315, People's Republic of China*

[2]*CAS Center for Excellence and Synergetic Innovation Center in Quantum Information and Quantum Physics, Shanghai Branch, University of Science and Technology of China, Shanghai 201315, People's Republic of China*

[3]*Jinan Institute of Quantum Technology, Jinan 250101, People's Republic of China*

[4]*Stanford Institute for Theoretical Physics, Stanford University, Stanford, California 94305, USA*

[5]*Center for Theoretical Physics, MIT, Cambridge, Massachusetts 02139, USA*

[6]*T. D. Lee Institute, Shanghai Jiao Tong University, Shanghai 200240, People's Republic of China*

[7]*Wilczek Quantum Center, School of Physics and Astronomy, Shanghai Jiao Tong University, Shanghai 200240, People's Republic of China*

[8]*Department of Physics, Stockholm University, Stockholm SE-106 91 Sweden*

[9]*Department of Physics and Origins Project, Arizona State University, Tempe, Arizona 25287, USA*

(Received 15 July 2019; published 9 December 2019)

By engineering and manipulating quantum entanglement between incoming photons and experimental apparatus, we construct single-photon detectors which cannot distinguish between photons of very different wavelengths. These color-erasure detectors enable a new kind of intensity interferometry, with potential applications in microscopy and astronomy. We demonstrate chromatic interferometry experimentally, observing robust interference using both coherent and incoherent photon sources.

DOI: 10.1103/PhysRevLett.123.243601

Quantum interference [1], which lies at the heart of quantum theory, requires complete indistinguishability between two particles. This is to say, as long as one can distinguish two particles even in principle, quantum interference will not happen. Meanwhile, quantum mechanics tells us if we can erase the two particles' past [2], interference will be restored. It has been shown that path or polarization information can be easily erased, while the frequency difference is generally hard to eliminate. For photons, conventional optical detectors are fundamentally photon counters, whose operation depends upon processes which are sensitive to the photons' energy. Thus, conventional detectors distinguish between different wavelengths, and therefore optical interference normally involves quasimonochromatic light [3]. Yet relative phases between photons of different wavelengths potentially provide a rich source of information. It is quite astonishing that, theoretically, the frequency information can be erased [4]. Here, we leveraged frequency-space entanglement to develop color-erasure detectors and achieve intensity interferometry [5,6] between light of very different wavelengths experimentally, thus revealing new features of optical radiation fields. This new type of interferometer might find immediate applications in astronomy, microscopy, and metrology [7–9].

Since the final stage of optical detection generally involves quantized processes, i.e., absorption or inelastic scattering, it is appropriate to use the language of photons. Consider two sources S_1, S_2 which emit photons of different colors γ_1, γ_2 which are received at detectors A, B. Simultaneous firing of A, B can be achieved in two ways: γ_1 excites A and γ_2 excites B, or γ_2 excites A and γ_1 excites B. If those two possibilities can be distinguished, then there is no interference between them. But if the detector can erase the color information of incoming photons, then interference will occur. Let us emphasize that according to the principles of quantum theory, interference only occurs if the two final states are strictly indistinguishable. Such strict color blindness cannot be achieved simply by ignoring color information. Rather, one must erase it. To do that we entangle the photons to the detectors using nonlinear processes [4].

In particular, we generate entanglement between an incoming γ_1 or γ_2 photon and a color-erasure detector. If the difference in energy between γ_1 and γ_2 is ΔE, then a color-erasure detector implements an entangling unitary of the form

$$\begin{aligned}|\gamma_1\rangle|\text{detector}\rangle &\longrightarrow \frac{1}{\sqrt{2}}|\gamma_1\rangle|\text{detector, measured}\gamma_1\rangle \\ &+ \frac{1}{\sqrt{2}}|\gamma_2\rangle|\text{detector} - \Delta E, \text{measured}\gamma_2\rangle \\ |\gamma_2\rangle|\text{detector}\rangle &\longrightarrow -\frac{1}{\sqrt{2}}|\gamma_1\rangle|\text{detector} + \Delta E, \text{measured}\gamma_1\rangle \\ &+ \frac{1}{\sqrt{2}}|\gamma_2\rangle|\text{detector, measured}\gamma_2\rangle \qquad (1)\end{aligned}$$

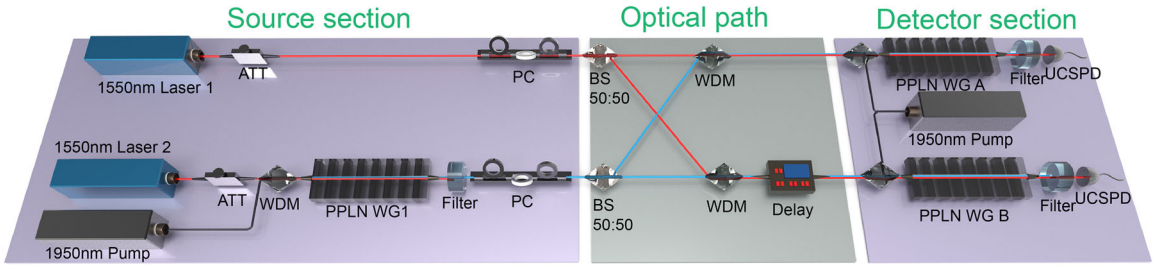

FIG. 1. Diagram of the chromatic intensity interferometer. VOA, variable optical attenuator; PPLN, periodically poled lithium niobate; BPF, an 863 nm bandpass filter; PC, polarization controller; BS, beam splitters; WDMs, two wavelength division multiplexers; UCSPDs, up-conversion single-photon detectors.

where $|\text{detector}\rangle$ is the initial state of the detector, $|\text{detector}, \text{measured}\gamma_1\rangle$ is the state of the detector having measured a γ_1 photon, $|\text{detector} + \Delta E, \text{measured}\gamma_1\rangle$ is the state of the detector having gained an energy ΔE and also having measured a γ_1 photon, and the other states are defined similarly. If we only consider occurrences where γ_1 is measured (i.e., project onto final states with a $|\gamma_1\rangle$), then we are left with either

$$|\gamma_1\rangle|\text{detector}, \text{measured}\gamma_1\rangle \quad \text{or}$$
$$|\gamma_1\rangle|\text{detector} + \Delta E, \text{measured}\gamma_1\rangle \tag{2}$$

the first state having come from an initial γ_1 photon and the second state having come from an initial γ_2 photon. The key point is that the overlap of the final detector states is approximately 1, namely

$$\langle \text{detector}, \text{measured}\gamma_1|\text{detector} + \Delta E, \text{measured}\gamma_1\rangle \approx 1, \tag{3}$$

and so our two final states in Eq. (2) are essentially indistinguishable, regardless of whether the initial incoming photon was γ_1 or γ_2. In other words, by generating a specific kind of entangled state between the incoming photon and the detector, we can cause decoherence (via our projective measurement) to quantum mechanically erase the color information of the initial photon. More details about these entangled states can be found in the Supplemental Material [10].

Our color-erasure detectors are technically and conceptually distinct from previous experiments in frequency-space interferometry. Conventional interferometry experiments, such as Mach-Zehnder and Hong-Ou-Mandel interferometry, are performed with standard beam splitters, but can equally well be performed with light beams of distinct polarization and polarizing beam splitters. In this spirit, recently more sophisticated experiments [18,19] performed Mach-Zehnder and Hong-Ou-Mandel interferometry with light beams of distinct frequency and frequency-space beam splitters. By contrast, color-erasure detectors retroactively recover interference from conventional interferometry experiments performed with standard beam splitters but distinct frequencies of light. This is akin to quantum eraser experiments [20,21], but now involving erasure of color information. An important advantage of our approach is that only the detection apparatus requires augmentation. This is convenient in general, and essential for imaging tasks involving self-luminous sources.

We realize chromatic intensity interferometry with our color-erasure detectors. As shown in Fig. 1, we first choose an attenuated 1550 nm laser as the source of γ_1. With the help of an 1950 nm pump laser, we up-convert another independent 1550 nm laser light into 863 nm light via sum-frequency generation in a home-made straight periodically poled lithium niobate (PPLN) waveguide [22] (PPLN WG1). An 863 nm bandpass filter is exploited to block the 1950 nm pump and the 863 nm light is taken as the source of γ_2. We then use beam splitters and wavelength division multiplexing (WDM) to divide and couple photons from both sources to the color-erasure detectors, which are composed of two integrated PPLN waveguides (PPLN WG A,B) [23], a 1950 nm pump source, bandpass filters, and two telecom band single-photon detectors [22].

In order to observe color-erasure interference, we need to change the relative phase between the γ_1 and γ_2 photons in one arm of the detector [4]. Since the phase of a γ_2 photon changes faster than that of a γ_1 photon with the same delay time, we can control the relative phase by adjusting the optical fiber delay (MDL-002) before detector B. We can choose the final output of the color-erasure detectors to be either γ_1 or γ_2, contingent on our choice of bandpass filters. We record the arrival time of each photon by a time-digital converter (TDC) and a computer.

Generally, intensity interferometry is observed in terms of $g^{(2)}(\tau)$, the second-order quantum mechanical correlation function. As we can see in the red curve in Fig. 2(a), the correlation $g^{(2)}(\tau = 3\ \text{ns})$ oscillates as we change the optical delay and detect γ_1 photons by filtering out the γ_2 photons. Photons from lasers obey Poissonian number statistics so that the τ average of $g^{(2)}(\tau)$ is 1.

The visibility of the interference is around 0.4, slightly less than the theoretically expected visibility 0.5 mainly due to the up-conversion single-photon detector's dark counts and baseline error from imperfect devices. For comparison, we also measure $g^{(2)}(\tau)$ without the pump

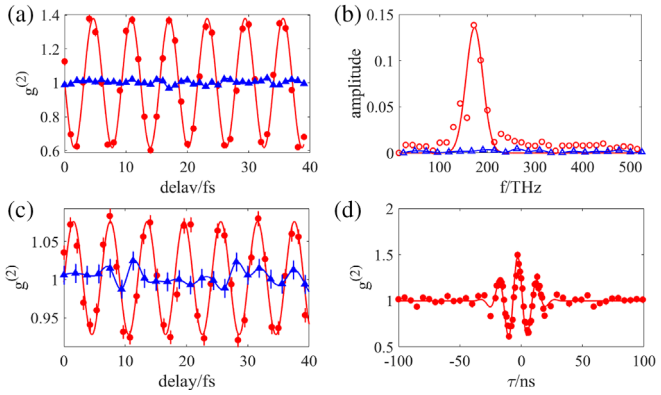

FIG. 2. Chromatic intensity interferometry of lasers. (a) $g^{(2)}(\tau = 3\ \mathrm{ns})$ as a function of the optical delay time, where the color-erasure detectors each output 1550 nm light. The red rounded markers display interference of different wavelengths of light due to the color-erasure detectors, whereas the blue triangle markers do not display interference since standard detectors are used. The same color scheme is used in (b) and (c). (b) The Fourier transform of $g^{(2)}(\tau = 3\ \mathrm{ns})$ as a function of the optical delay time. (c) $g^{(2)}(\tau = 3\ \mathrm{ns})$ as a function of the optical delay time, where the color-erasure detectors each output 863 nm light. (d) $g^{(2)}(\tau)$ as a function of the delay τ between the two detectors.

light. As expected, the interference pattern disappears, as shown by the blue curve of Fig. 2(a).

Figure 2(b) shows the Fourier transforms of the two curves in Fig. 2(a). The location of the peak of the red curve represents the frequency of the interference pattern, i.e., the rate of phase change as we scan the optical delay. In our case, the rate of phase change is theoretically the frequency of pump. The measured peak position is around 144 THz, which well coincides with 1950 nm. The blue curve in Fig. 2(b) is just noise and so has no large peaks, demonstrating that interference does not occur in the absence of color-erasure detectors.

Instead of having each color-erasure detector output 1550 nm light, we can instead arrange that the detectors each output 863 nm light. Data for this alternative arrangement are shown in Fig. 2(c). In the figure, we filter in only γ_2 photons at the output of the waveguides, and collect coincidence counts with and without the pumps enabling color-erasure detection. Relative to filtering in γ_1 photons, the visibility of interference when filtering in γ_2 photons is degraded since the photons tend to be multimode when propagating through the PPLN waveguides comprising our color-erasure detectors. Only photons in the lowest transverse mode participate in interference. The photons in other modes induce noise and thus reduce the visibility.

We also perform Hong-Ou-Mandel interference [24] utilizing standard beam splitters and two different wavelengths of light. The interference can only be recovered with color-erasure detectors. Instead of changing the relative time delay of the light beams, we instead observe coincidence counts between different time slots in the TDC. In Fig. 2(d), we observe an oscillation of $g^{(2)}(\tau)$ as a function of τ, which decays as the delay between two detectors surpasses the coherence time of the light sources. We can produce bunching or antibunching depending on the setup of the interferometer, and the settings of the color-erasure detectors.

In a tabletop demonstration experiment, it is convenient to use lasers as light sources. Considering future applications, we would like to observe chromatic interferometry for incoherent or semi-incoherent sources such as thermal light from a star or photon emission from fluorescent proteins. Therefore, it is important to demonstrate that our chromatic intensity interferometer can function with thermal light. Accordingly, we experimentally performed chromatic intensity interferometry with thermal light sources. To construct a thermal source, we prepare a C band amplified spontaneous emission (ASE) light source with 30 nm spectral bandwidth. We first filter the ASE light with a 100 GHz bandwidth dense wavelength division multiplexer and then amplify it with an erbium doped fiber amplifier (EDFA). The emission of EDFA is further filtered by a 50 MHz bandwidth etalon to select out a thermally populated mode which is then divided into two beams. One is used for γ_1 and the other one is converted to 863 nm in a PPLN waveguide to become γ_2, similar to the coherent laser setting from before. In this thermal source setup, the γ_1 and γ_2 photons are generated from the same source and thus their phases are correlated. To destroy these correlations, the γ_1 beam is sent through a 20 km spool of fiber, and fluctuations of the fiber ruin the phase coherence between γ_1 and γ_2. Then we send both beams to the color-erasure detectors and observe interference.

As shown in Figs. 3(a) and 3(c), we observed interference of the thermal light in when the color-erasure detectors output only $|\gamma_1\gamma_1\rangle$ or only $|\gamma_2\gamma_2\rangle$, respectively. We also compute the Fourier transform of the interference pattern for the $|\gamma_1\gamma_1\rangle$ case. In the absence of color-erasure detectors (i.e., by not pumping the waveguides), we check that interference does not occur. We have also performed chromatic Hong-Ou-Mandel interferometry with these thermal sources, and $g^{(2)}(\tau)$ is shown in Fig. 3(d).

One apparent difference between our experimental data for thermal sources vs coherent lasers is the mean value of the interference patterns. In Figs. 3(a) and 3(c), the mean value is larger than 1, which coincidences with the super-Poissonian number statistics of thermal light. The visibility for the thermal sources is worse than for the coherent lasers since the coherence time of the thermal sources is much shorter. Thus, every mismatch in the optical path will lead to the loss of coherence and visibility.

Since we expect color-erasure detectors to have applications in free space imaging, we also performed chromatic interferometry in free space. As shown in Fig. 4(a), we detect the photons from two disklike sources emitting different wavelengths of light.

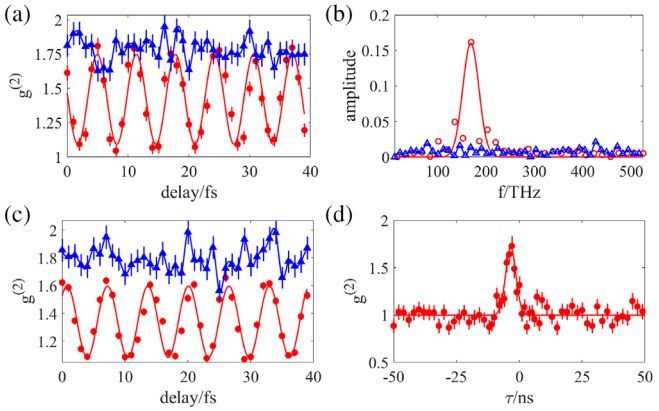

FIG. 3. Chromatic intensity interferometry of thermal sources. (a) $g^{(2)}(\tau)$ for $\tau \approx 0$ as a function of the optical delay time, where the color-erasure detectors each output 1550 nm light. The red rounded markers show interference due to the aid of the color-erasure detectors, whereas the blue triangle markers show the null outcome in the absence of color-erasure detectors. This color scheme is also used in (b) and (c). (b) The Fourier transform of $g^{(2)}(\tau)$ for $\tau \approx 0$ as a function of the optical delay time. (c) $g^{(2)}(\tau)$ for $\tau \approx 0$ as a function of the optical delay time, where the color-erasure detectors each output 863 nm light. (d) $g^{(2)}(\tau)$ as a function of the delay τ between the two detectors.

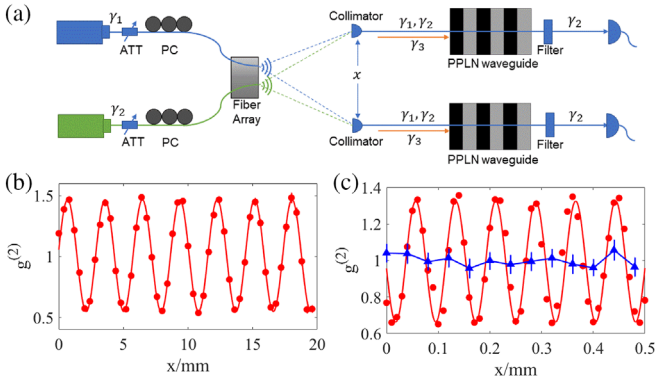

FIG. 4. Chromatic intensity interferometry in free space. (a) A diagram of the experimental setup for the intensity interferometer in free space. Lasers from a fiber array are utilized as sources, and the collimators are utilized to couple light from free space into color-erasure detectors. One of the collimators is mounted on a linear translation stage to control the distance x between the two collimators. (b) The measured interference pattern when both sources emit light of the same wavelength, reproducing standard Hanbury Brown and Twiss interference. (c) The measured interference pattern when the two sources emit 1550 and 863 nm light, respectively. The red rounded markers show interference due to the aid of the color-erasure detectors, whereas the blue triangle markers show the absence of interference without the color-erasure detectors.

The disklike sources are situated 125 μm apart in a fiber array, and color-erasure detectors are placed 40 cm away. When we move the position of one of the detectors using a linear translation stage, we observe an interference pattern, as shown in the red curve in Fig. 4(c). The blue curve in Fig. 4(c) illustrates that interference is not observed in the absence of color-erasure detection. We also show in Fig. 4(b) the standard Hanbury Brown and Twiss interference pattern when the two sources emit at the same wavelength, utilizing standard detection apparatus. Our free space results for chromatic interferometry demonstrate the potential application of color-erasure detection in imaging.

In conclusion, we have used our color-erasure detectors to perform intensity interferometry between photons of very different wavelengths, and to recover their relative phase information, which is inaccessible to conventional detectors. Since our technique does not require lenses, it could be used with very large apertures, and in regions of the spectrum where lenses are not readily available. This might inspire new opportunities for imaging and thus calls for further theoretical and experimental research. As an example, color-erasure detectors can enhance the ability of fluorescent microscopes [25,26] to resolve nearby proteins which emit at distinct frequencies. We can also leverage a generalization of the van Cittert–Zernike formula for sources of different wavelengths measured with color-erasure detectors [4].

If instead we had a nearly perfect single-photon detector, which has no noise, no jitter, no dead time, and is very fast, we can effectively erase the frequency of incoming photons and use it in the multicolor Hanbury Brown–Twiss interferometer. However, there does not exist a photon detector or traditional photodiode faster than 144 THz, as would be required in our experiment. What is more, a fast detector acts like a very narrow timing filter, which filters the two input light pulses into a very narrow time window. This would filter out most of the photons in the pulses. In our experiment, the linewidth for the input laser is around 3 MHz and the detector bandwidth is around 144 THz. Only around 0.002% (3 MHz/144 THz) of the light will be detected. In this sense, it is indeed inefficient. Meanwhile, our system can convert photons with an efficiency of around 50% which is orders of magnitude higher than a fast detection method. This is actually not due to a technological advance but a difference in concept. Instead of filtering light, we coherently convert different wavelengths of light to become indistinguishable.

Our work exploits and emphasizes the realization that detectors are themselves quantum mechanical objects, which "measure" other systems by becoming entangled with them [4,27,28]. Indeed, the core mechanism enabling multiwavelength intensity interferometry is a trade-off between coherence of multiphoton phase information and coherence of color information, implemented by crafting and manipulating the entanglement between source photons and the detection apparatus. (For mathematical details, see the Supplemental Material [10].) We anticipate that further analysis of the quantum mechanics of detectors will reveal other trade-off opportunities.

We would like to thank Andreas Kaldun and Philip Bucksbaum for valuable conversations and thank Lian-Tuan Xiao and Jian-Yong Hu for lending equipment. This work was supported by the National Key R&D Program of China (No. 2018YFB0504300), the National Natural Science Foundation of China, the Chinese Academy of Science, and the Swedish Research Council. J. C. is supported by the Fannie and John Hertz Foundation and the Stanford Graduate Fellowship program. The work of F. W. is supported by the Swedish Research Council under Contract No. 335-2014-7424, the U.S. Department of Energy under grant Contract No. DE-SC0012567, and by the European Research Council under Grant No. 742104.

L.-Y. Q., J. C., and F. M. contributed equally to this work.

[1] P. Hariharan, *Basics of Interferometry* (Elsevier, Amsterdam, 2010).
[2] M. O. Scully and K. Drühl, Phys. Rev. A **25**, 2208 (1982).
[3] L. Mandel and E. Wolf, *Optical Coherence and Quantum Optics* (Cambridge University Press, Cambridge, England, 1995).
[4] J. Cotler, F. Wilczek, and V. Borish, arXiv:1607.05719.
[5] R. H. Brown and R. Twiss, Nature (London) **178**, 1046 (1956).
[6] G. Baym, Acta Phys. Pol. Ser. B **29**, 1839 (1998).
[7] J. D. Monnier, Rep. Prog. Phys. **66**, 789 (2003).
[8] G. Shtengel, J. A. Galbraith, C. G. Galbraith, J. Lippincott-Schwartz, J. M. Gillette, S. Manley, R. Sougrat, C. M. Waterman, P. Kanchanawong, M. W. Davidson *et al.*, Proc. Natl. Acad. Sci. U.S.A. **106**, 3125 (2009).
[9] V. Giovannetti, S. Lloyd, and L. Maccone, Nat. Photonics **5**, 222 (2011).
[10] See Supplemental Material at http://link.aps.org/supplemental/10.1103/PhysRevLett.123.243601 for theoretical overview, how color information be erased, and experimental details, which includes Refs. [11–17].
[11] K. R. Parameswaran, R. K. Route, J. R. Kurz, R. V. Roussev, M. M. Fejer, and M. Fujimura, Opt. Lett. **27**, 179 (2002).
[12] R. Ikuta, Y. Kusaka, T. Kitano, H. Kato, T. Yamamoto, M. Koashi, and N. Imoto, Nat. Commun. **2**, 537 (2011).
[13] K. De Greve, L. Yu, P. L. McMahon, J. S. Pelc, C. M. Natarajan, N. Y. Kim, E. Abe, S. Maier, C. Schneider, M. Kamp *et al.*, Nature (London) **491**, 421 (2012).
[14] M. Chou, J. Hauden, M. Arbore, and M. Fejer, Opt. Lett. **23**, 1004 (1998).
[15] A. P. Vandevender and P. G. Kwiat, J. Mod. Opt. **51**, 1433 (2004).
[16] L. Ma, O. Slattery, and X. Tang, Opt. Express **17**, 14395 (2009).
[17] P. Kumar, Opt. Lett. **15**, 1476 (1990).
[18] T. Kobayashi, R. Ikuta, S. Yasui, S. Miki, T. Yamashita, H. Terai, T. Yamamoto, M. Koashi, and N. Imoto, Nat. Photonics **10**, 441 (2016).
[19] T. Kobayashi, D. Yamazaki, K. Matsuki, R. Ikuta, S. Miki, T. Yamashita, H. Terai, T. Yamamoto, M. Koashi, and N. Imoto, Opt. Express **25**, 12052 (2017).
[20] M. O. Scully, B.-G. Englert, and H. Walther, Nature (London) **351**, 111 (1991).
[21] P. G. Kwiat, A. M. Steinberg, and R. Y. Chiao, Phys. Rev. A **45**, 7729 (1992).
[22] M.-Y. Zheng, G.-L. Shentu, F. Ma, F. Zhou, H.-T. Zhang, Y.-Q. Dai, X. Xie, Q. Zhang, and J.-W. Pan, Rev. Sci. Instrum. **87**, 093115 (2016).
[23] F. Ma, L.-Y. Liang, J.-P. Chen, Y. Gao, M.-Y. Zheng, X.-P. Xie, H. Liu, Q. Zhang, and J.-W. Pan, J. Opt. Soc. Am. B **35**, 2096 (2018).
[24] C.-K. Hong, Z.-Y. Ou, and L. Mandel, Phys. Rev. Lett. **59**, 2044 (1987).
[25] O. Schwartz, J. M. Levitt, R. Tenne, S. Itzhakov, Z. Deutsch, and D. Oron, Nano Lett. **13**, 5832 (2013).
[26] B. O. Leung and K. C. Chou, Appl. Spectrosc. **65**, 967 (2011).
[27] W. H. Zurek, Rev. Mod. Phys. **75**, 715 (2003).
[28] W. H. Zurek, Nat. Phys. **5**, 181 (2009).